Experimental investigation on CFRP-to-concrete bonded joints across crack

Özgür Anil[1]*, Çağatay M. Belgin[1] and M. Emin Kara[2]

[1]Civil Engineering Department, Gazi University, Maltepe, Ankara 06570, Turkey
[2]Civil Engineering Department, Aksaray University, Aksaray, Turkey

Abstract. Bonding of carbon fiber reinforced polymer (CFRP) composites has become a popular technique for strengthening concrete structures in recent years. The bond stress between concrete and CFRP is the main factor determining the strength, rigidity, failure mode and behavior of a reinforced concrete member strengthened with CFRP. The accurate evaluation of the strain is required for analytical calculations and design processes. In this study, the strain between concrete and bonded CFRP sheets across the notch is tested. In this paper, indirect axial tension is applied to CFRP bonded test specimen by a four point bending tests. The variables studied in this research are CFRP sheet width, bond length and the concrete compression strength. Furthermore, the effect of a crack- modeled as a notch- on the strain distribution is studied. It is observed that the strain in the CFRP to concrete interface reaches its maximum values near the crack tips. It is also observed that extending the CFRP sheet more than to a certain length does not affect the strength and the strain distribution of the bonding. The stress distribution obtained from experiments are compared to Chen and Teng's (2001) analytical model.

1. Introduction

CFRP is being commonly used in the last 10 years because it is light in weight, easy to apply, resistant to corrosion and many environmental conditions, does not change the geometrical sizes of the elements and there are many different materials and dimensions in the market suitable for different kinds of strengthening details (Teng *et al.* 2002).

When the experimental studies in the literature were surveyed, three modes of failure where found for concrete structures strengthened with CFRP (Smith and Teng 2002a, b, 2003, Oehlers and Moran 1990, Teng *et al.* 2003, Mohamed *et al.* 2001, 2002, Oehlers *et al.* 2003). The observed failures are, debonding of CFRP from concrete (Type-I), epoxy failure due to shear stress exceeding shear strength of adhesive concrete interface (Type-II) and rupture of CFRP (Type-III). Since CFRP has very high tensile strength, CFRP rupture is a rare case. If this failure mode is encountered, the whole capacity of the CFRP is used, and this means that the aim of the strengthening has reached its goal. However often CFRP debonds from the concrete surface or the adhesive concrete interface when the shear stress reaches its shear stress capacity and fails before CFRP rupture. A common

---

*Corresponding author, Associate Professor, E-mail: oanil@gazi.edu.tr

failure mode is debonding of the CFRP to concrete just a couple of millimeters below the surface.

Required strengthening with CFRP can not be achieved due to debonding failure. The main factor affecting this type of failure is the compression strength of concrete which is one of the parameter in this study. The other two parameters are the CFRP sheet width and the bond length. The strength and the rigidity of the strengthened specimen depend on the failure mode. If the structure fails because of the debonding of CFRP (Type-I), the strain distribution between CFRP and the concrete must be known for calculating the capacity of the strengthened structure. Hence the studies of determining the strain between CFRP and the concrete became popular in the recent years (Chen 2001, Teng *et al.* 2002, Smith and Teng 2002a, b, 2003, Teng *et al.* 2003, Chen and Teng 2003, Yao *et al.* 2005, Jayaprakash *et al.* 2007). In all these studies the necessity of the knowledge of the distribution of the strain to calculate the capacity of the structure is emphasized. A recent survey (Yao *et al.* 2005) showed that many different experimental setups have been used for determining the CFRP-to-concrete bond strength, but no consensus on a standard test procedure has been reached. The existing work has included experimental studies conducted using single shear tests, e.g. (Bizindavyi and Neale 1997, Bizindavyi and Neale 1999, Chajes *et al.* 1996, Chajes *et al.* 1995, Taljsten 1997), double shear tests, e.g. (Brosens and van Gemert 1997, Fukuzawa *et al.* 1997, Hiroyuki and Wu 1997, Kobatake *et al.* 1993, Maeda *et al.* 1997, Neubauer and Rostásy 1997, Swamy *et al.* 1986, Van Gemert 1980) and modified beam tests, e.g. (Van Gemert 1980, De Lorenzis *et al.* 2001, Ziraba *et al.* 1995). The existing experimental setups were classified into the following five types: (a) double-shear pull tests; (b) double-shear push tests; (c) single-shear pull tests; (d) single-shear push tests; and (e) beam (or bending) tests (Yao *et al.* 2005), see also Fig. 1.

The first four experimental setups that were used for determining the strain distributions are very

(a) Double - shear pull tests   (b) Double - shear push tests

(c) Single - shear pull tests   (d) Single - shear push tests
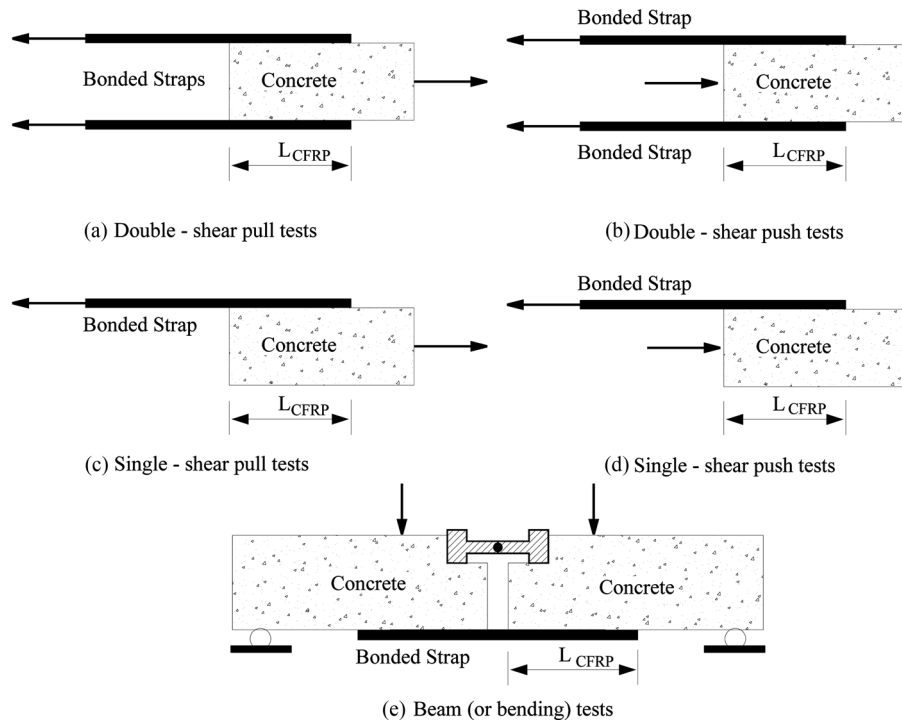
(e) Beam (or bending) tests

Fig. 1 Classification of experimental setup for evaluating of bond strength (Chen *et al.* 2001)

complicated, at which some special apparatus are utilized. All these complicated mechanical systems are added to the setup for applying an axial tension load to the CFRP accurately. But it is very complicated to apply pure axial tension load to the CFRP. On the other hand it is very rare to see a CFRP member experiencing only an axial tension load in the structures strengthened with CFRP. For example when a beam is strengthened in flexure, the CFRP is bonded to tension face of the beam (underside) and the CFRP is subjected to combined bending and tension simultaneously. Combined stress case is occurred usually in CFRP's which are used for repairing and strengthening applications.

When the concrete structure starts to crack, CFRP strain values start to rise and the CFRP begins to contribute to the strength and the rigidity of the strengthened structure. It is considered that when the crack occurs in the concrete under the CFRP sheets, the strain distribution in CFRP is affected significantly. The actual case is just the same as above mentioned. It is not possible to have a concrete without any cracks when the load is applied. As a result the strain distribution between CFRP and a notched concrete beam that was used for modeling a structure with a single crack is studied in this study. CFRP is bonded across the notch to determine the effect of the notch to the strain distribution in CFRP. With the evaluation of the experimental results, the effect of the three parameters mentioned above to the load-displacement and strain distributions of the concrete member strengthened with CFRP are studied. Experimental results are compared to Chen and Teng's (2001) analytical model and the comparison of experimental findings to the analytical model is studied.

2. Experimental programme

2.1 Test specimens and materials

In this study sixteen notched concrete beams were casted and tested under monotonic loading. No reinforcement was used in the beams. The geometrical shapes of the test specimens are given in Fig. 2. The beams were casted with a 20 mm wide and 50 mm deep notch to model a crack in the

Notes : L_{CFRP}: Bonding length of CFRP = 120, 180, 240 and 300 mm

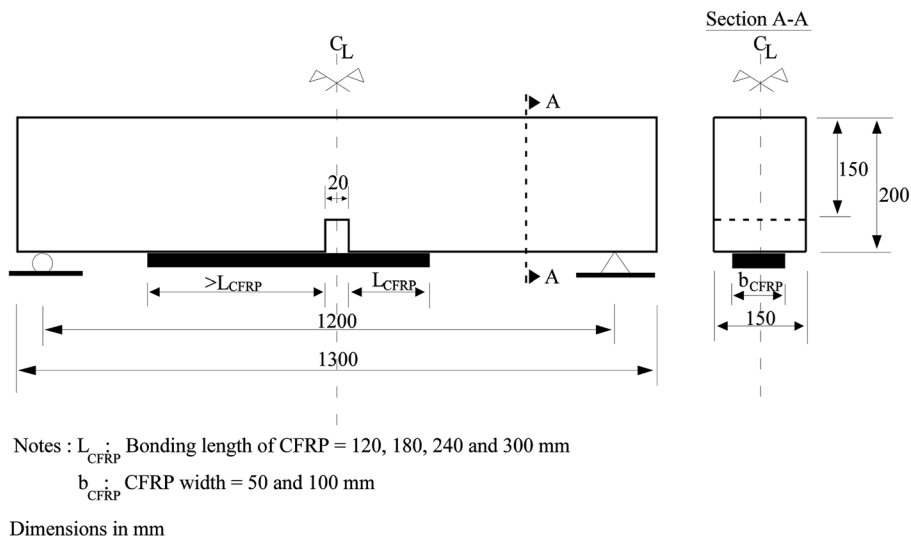b_{CFRP}: CFRP width = 50 and 100 mm

Dimensions in mm

Fig. 2 Details of test specimens

beam to evaluate the effect of a crack to the strain distribution between CFRP and concrete. The notch was placed at the center of the span, on the symmetry axis. The cross-section of the concrete beams was 150×200 mm and the span between the supports was 1200 mm. The load was applied monotonically with a four point loading arrangement.

The properties of the test specimens are given in Table 1. In the study a total of 16 beams were casted (2×4×2) with two different width and four different bonding lengths of the CFRP sheets and with two different types of concrete qualities, one concrete with 15 MPa and one with 25 MPa compressive strength, respectively. The compressive strengths of the test beams tested by standard cylindrical compression test, are given in Table 1. The admixture ratios of the two different concrete

Table 1 Properties of specimens

Specimen #	Average compression strength of concrete f_C (MPa)	CFRP sheet width b_{CFRP} (mm)	CFRP sheet bonding length L_{CFRP} (mm)
1	15.2		120
2	14.8	50	180
3	14.4		240
4	15.6		300
5	15.8		120
6	14.2	100	180
7	14.7		240
8	15.3		300
9	25.0		120
10	26.0	50	180
11	24.0		240
12	25.2		300
13	24.8		120
14	24.4	100	180
15	25.6		240
16	25.0		300

Table 2 Mixture design of concrete

Target average compression strength of concrete	Material	Percentage by Weight (%)
15	0-7 mm Aggregate	49
	7-15 mm Aggregate	33
	Cement	9
	Water	9
25	0-7 mm Aggregate	30
	7-15 mm Aggregate	45
	Cement	17
	Water	8

are given in Table 2. In the tests, 50 mm and 100 mm wide CFRP sheets were used with 120 mm, 180 mm, 240 mm, and 300 mm bonding lengths.

All the beams with the same concrete compressive strength were casted from the same admixture, and at the same time. All the beams were cured in identical conditions for the first 14 days and left for drying for another 14 days. All the beams were ready for bonding the CFRP sheets after 28 days. CFRP sheets were bonded to the concrete beams according to the experimental procedure previously determined. The sheets were bonded to the symmetry axis of the cross-section of the beam. Strain-
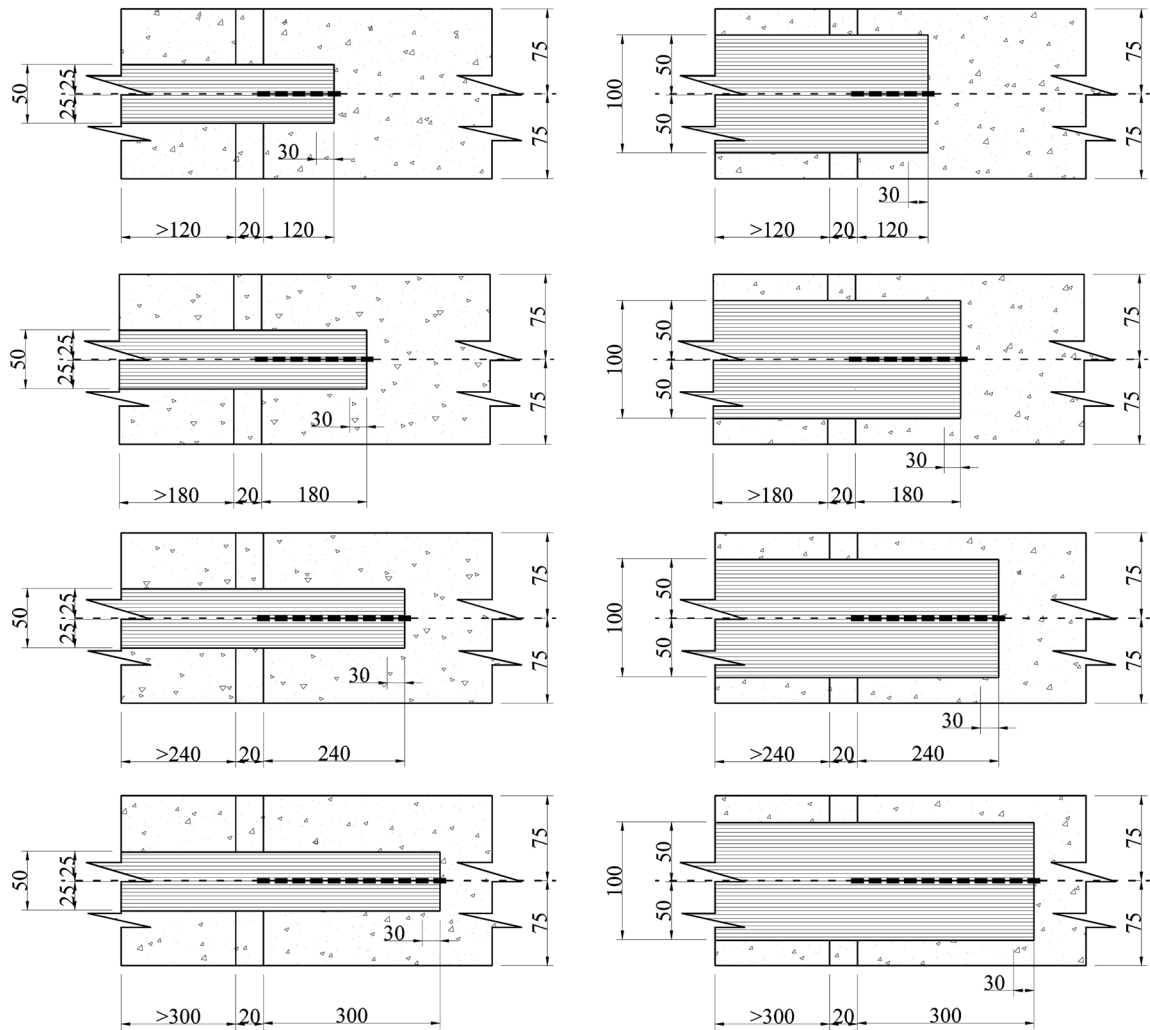
(a) Layout for 50 mm width CFRP and position of strain gauges

(b) Layout for 100 mm width CFRP and position of strain gauges

Dimensions in mm

Fig. 3 CFRP sheet layout and details

gauges were attached to CFRP along the one side of notch with 30 mm spacing. The other side of the CFRP was kept longer to maintain a failure on the strain-gauge attached side. The details of the bonded CFRP and the locations of the strain-gauges are given in Fig. 3.

2.2 Bonding procedure

The bonding procedure adopted was according to the CFRP and epoxy manufacturer's application guide. Unidirectional CFRP (Sikawrap230C® of the Sika®) and, two component epoxy (Sikadur 330®) were used. The properties of these materials are given in Table 3.

Before bonding CFRP members on the concrete surface, special attention was given to the beam surface preparation. Bottom surface of the beam were roughed by a mechanical grinding machine until the aggregate was exposed and then brushed and surface vacuumed to remove all the loose particles and dust. Later, the epoxy resin was mixed in accordance with manufacturer's instruction. Mixing was carried out in a metal container and was kept on until the mixture obtained a uniform color. The prepared epoxy resin (Sikadur 330®) was applied to the surface of the concrete where the CFRP will be bonded. Then the CFRP sheet (Sikawrap230C®) was laid on to the epoxy resin and pressed thoroughly to obtain the absorption of the resin by the fiber material and to obtain a bubble free interface between CFRP and concrete. Finally the CFRP was covered with another layer of epoxy resin for protection. The temperature during the application was 20 ± 2°C. The beams were tested after 14 days of CFRP bonding. The photos of the CFRP bonded concrete beams before test are given in Fig. 4.

2.3 Experimental setup

The tests were carried out in a closed frame with a capacity of 400 kN. The monotonic load was applied with a 300 kN capacity hydraulic jack. The experimental and the measurement setup are given in Fig. 5. In all specimens, the ratio of shear span (a = 400 mm) to the effective depth (d =

Table 3 Properties of CFRP and resin

Properties of CFRP	Remarks of CFRP
Construction	Warp : Carbon Fibers (99% of total areal weight)
	Weft : Thermoplastic heat-set fibers (1% of total areal weight)
Areal Weight (g/m^2)	220±10
Density (g/m^3)	1.78×10^{-6}
Thickness (mm)	0.12
Tensile Strength (MPa)	4100
Elastic Modulus (MPa)	231000
Ultimate Tensile Strain (%)	1.7%
Properties of Resin	Remarks of Resin
Tensile Strength (MPa)	30
Elastic Modulus (MPa)	3800

Remarks: This information were given by manufacturer

(a) A view of bonding of CFRP sheet
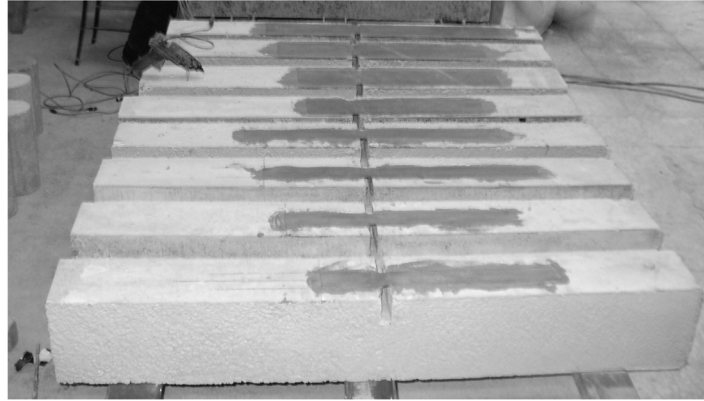
(b) Test specimen prepared for testing

Fig. 4 Photograph of specimens before test

200 mm) was identical ($a/d = 2$). A load-cell with a capacity of 400 kN was used for measuring the applied load during the experiments. The vertical displacements of the supports and the midpoint of the beam were measured by displacement transducers (Linear Variable Differential Transformers (LVDT)). The beam midpoint net displacements of the beam due to bending were calculated using the vertical displacements of the supports. The tests were carried out with the observation of the load-midpoint displacement graph sketched simultaneously on the monitor by using measurements of load-cell and LVDTs. The load was increased until the beams failed.

Strain-gauges of 120Ω, and 15 mm gauge length were attached on the CFRP sheets starting from the side of the notch every 30 mm interval in order to measure the strain level at the CFRP strip. All measurements were carried out with computerized data logger during the experiments. Total 5, 7, 9 and 11 strain values were recorded from 120 mm, 180 mm, 240 mm and 300 mm long bonded CFRP sheets, respectively. Strain-gauges were attached symmetrically to the CFRP sheet axis and along the main fiber direction.
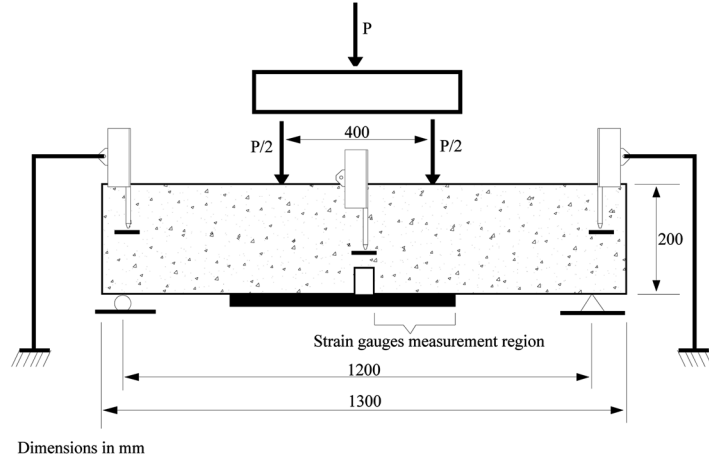
(a) Schematic view of test setup and instrumentations
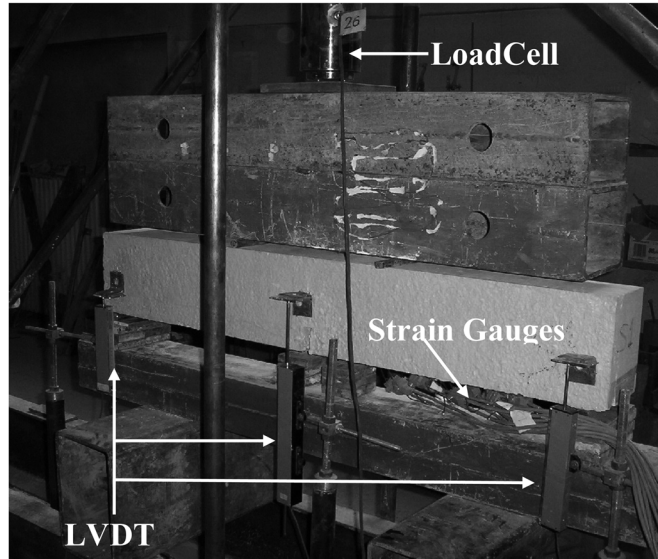
(b) Photograph of test setup

Fig. 5 Test setup and instrumentation

3. Experimental results and evaluations

3.1 Load-displacement behavior and failure modes

The load-displacement graphs of the test specimens are given in Fig. 6. In four-point bending, the shear force equals half the total transverse load. The main parameter affecting the ultimate load capacity of the specimens is found to be the CFRP sheet width when the load-displacement graphs are examined. It could be seen that the bond length of the CFRP sheet and the compressive strength of concrete had less effect on the ultimate load capacity of the specimens than the CFRP width. The
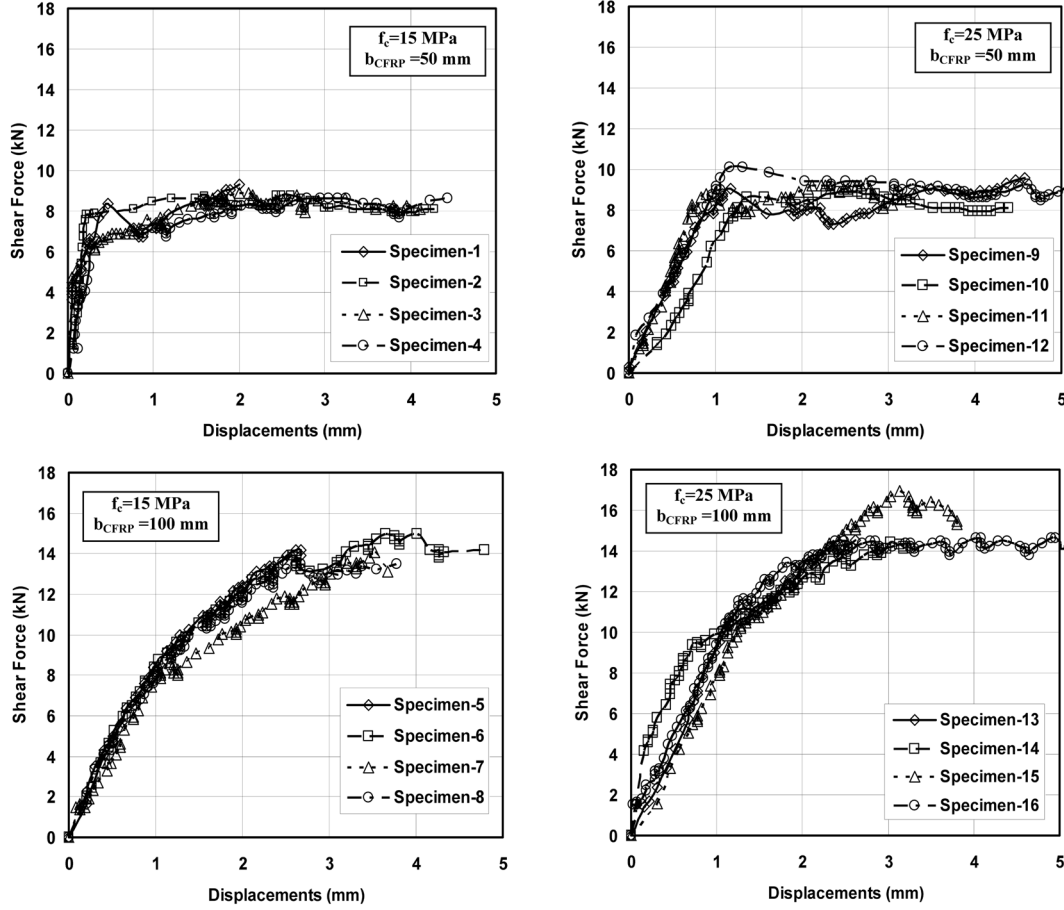
Fig. 6 Load-displacement graph of specimens

100 mm wide CFRP sheets increased the ultimate load capacity of the specimen on an average of 59% more than 50 mm wide CFRP sheets. The CFRPs with different bond lengths have close ultimate load values. It is found that the ultimate load capacity of the specimen that had 50 mm wide CFRP sheet, and 15 MPa concrete compressive strength is 6% less than the specimen that had same CFRP sheet width, and 25 MPa concrete compressive strength. The difference is calculated as 7% in the specimens with 100 mm CFRP sheet width. All of the test results are summarized in Table 4.

Two types of failure modes were observed during the experiments. One of which was debonding of the CFRP with the concrete just a couple of millimeters above the bottom surface of the concrete (Type-I), and the other one was the failure of the adhesive concrete interface due to the load exceeding the shear strength of the epoxy resin (Type-II). Specimens 1, 2, and 6 failed due to failure of epoxy resin with excessive shear loading, whereas the others failed with the debonding of the CFRP with concrete due to the shear stresses exceeding of the shear strength of concrete. Some of the photos taken from the latter case are given in Fig. 7. Some observations are carried out on the specimens in the latter case. It is seen that the thickness of the debonded concrete is between 1.0-3.5 mm. The aggregates could be seen on the surface of debonding. The thickness differs with the change of the strain distribution. It is observed that near the notch mouth tip where the strains are

Table 4 Test results of specimens

Specimen #	Concrete compression strength f_C (MPa)	CFRP sheet		Ultimate load (kN)	Maximum strain in CFRP at ultimate load level ($\mu\varepsilon$)	Failure Modes
		Width (mm)	Bonding length (mm)			
1			120	9.3	4776	Debonding at adhesive concrete interface (Type-II)
2		50	180	8.8	4691	Debonding at adhesive concrete interface (Type-II)
3			240	8.9	5213	Debonding in concrete (Type-I)
4	15		300	8.7	5953	Debonding in concrete (Type-I)
5			120	14.2	5951	Debonding in concrete (Type-I)
6		100	180	15.0	4446	Debonding at adhesive concrete interface (Type-II)
7			240	14.1	5667	Debonding in concrete (Type-I)
8			300	13.5	6080	Debonding in concrete (Type-I)
9			120	9.6	5504	Debonding in concrete (Type-I)
10		50	180	8.9	5201	Debonding in concrete (Type-I)
11			240	9.3	5919	Debonding in concrete (Type-I)
12	25		300	10.1	5660	Debonding in concrete (Type-I)
13			120	14.5	5557.	Debonding in concrete (Type-I)
14		100	180	14.4	6026	Debonding in concrete (Type-I)
15			240	16.9	5499	Debonding in concrete (Type-I)
16			300	14.6	5880	Debonding in concrete (Type-I)

higher the debonding thickness of the concrete had reached its maximum values and coarse concrete pieces were debonded (Fig. 7). Also the thickness of the debonded concrete increases at the end of the CFRP sheet compared to the central region. However the thickness of the debonded concrete at the end is less compared to the one near the notch mouth tip. It is understand that the increase in the strain distribution is the main reason for the thicker debonding of concrete. This implies that the interfacial stresses are higher at the notch mouth tip as compared to the CFRP end.

Observing the specimens it could be seen that the debonding thickness of the concrete decreases and becomes uniform away from the notch mouth tip as the CFRP sheet bonding length increases. The debonding concrete thickness increases with the increasing CFRP sheet width. The thickness decreases at far away regions from the notch. Changing the CFRP sheet width and bond length changes the time periods to reach the ultimate capacity of the test specimens. A sudden failure was observed in the specimens with shorter CFRP bonding length. As the CFRP bonding length increased the cracks were easily observed due to elongated failure time. Therefore failure mode observed more easily.

The other type of failure observed in the specimens is the debonding of CFRP sheet due to failure
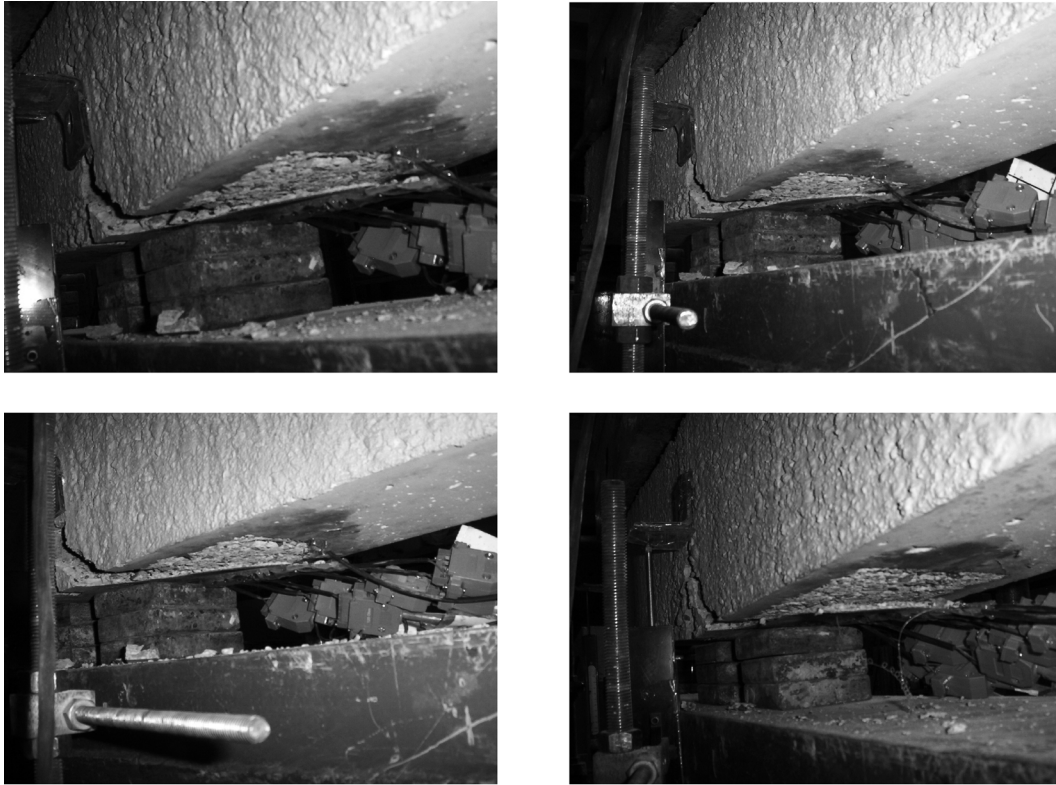
Fig. 7 Photograph of debonding failure in a specimen

of epoxy resin with excessive shear loading (Type-II). This type of failure occurred with the specimens which has a concrete compressive strength of 15 MPa. The strain values are much smaller in this case than the former failure mode (debonding of CFRP with concrete).

3.2 Strain distributions in CFRP sheet

The strain distribution of the specimens measured from the strain-gauges attached on the CFRP sheets are given in Fig. 8. In order to evaluate the changes in the strain distribution during loading, the strain values of five different load levels are given in the graphs. The load levels are given in the form of a fraction of ultimate load values. When the strain graphs are examined some common features that are independent from the experimental variables could be observed. The most evident feature is that the maximum strain value recorded at the ultimate load is always near the notch mouth tip. Another feature is that the strain values increased gradually up to 50% of the ultimate load whereas after this point the strain values increased rapidly.

In the debonding of the CFRP with concrete failure cases (Type-I), the mean strain value recorded at the level of ultimate load was 5700 $\mu\varepsilon$ whereas in the failure of epoxy resin cases (Type-II) the value recorded was 4640 $\mu\varepsilon$. The mean strain values at the ultimate load level are 23% higher in the debonding of the CFRP with concrete failure than the failure of epoxy adhesive cases.

In this section the effects of the experimental variables on the strain values are summarized. The
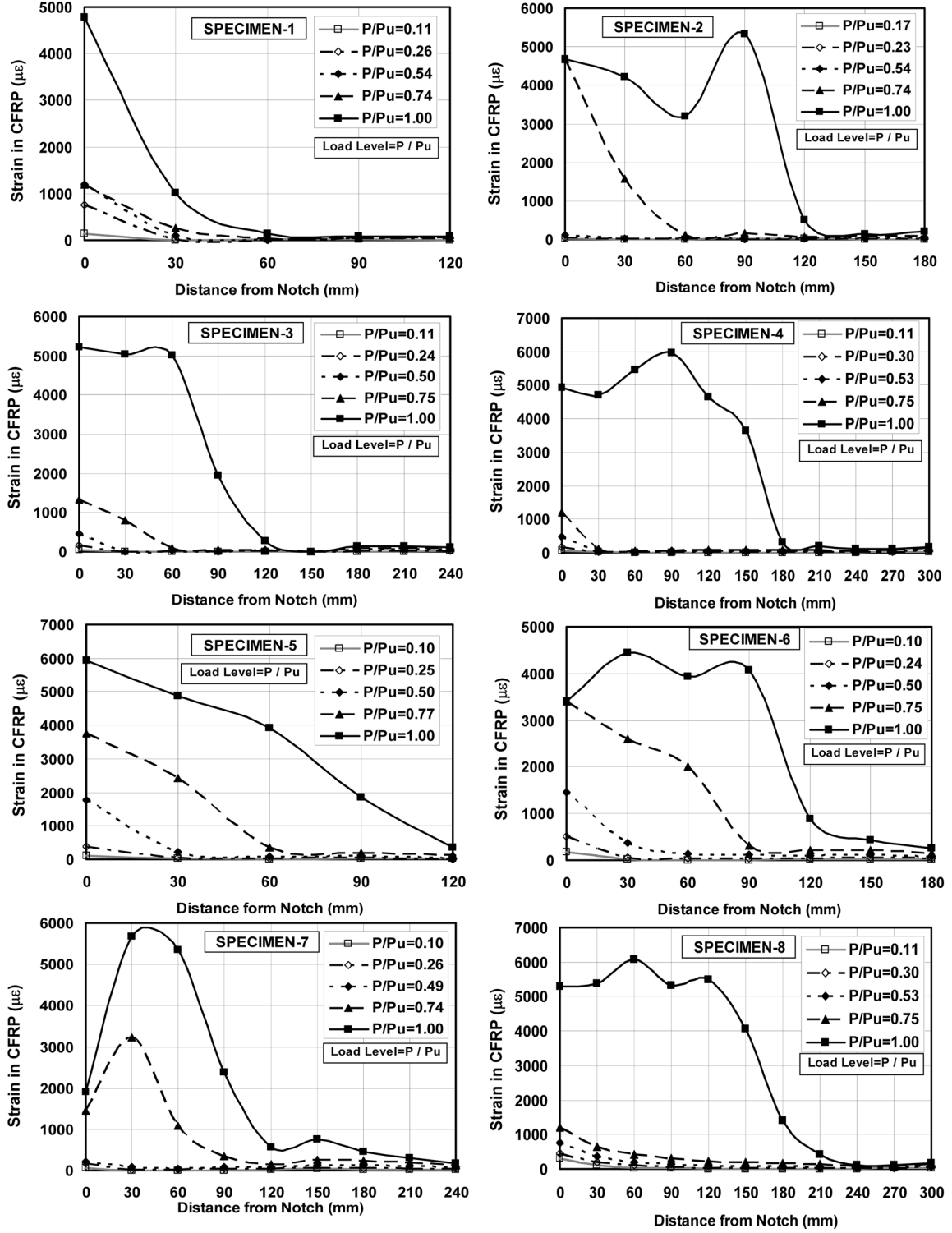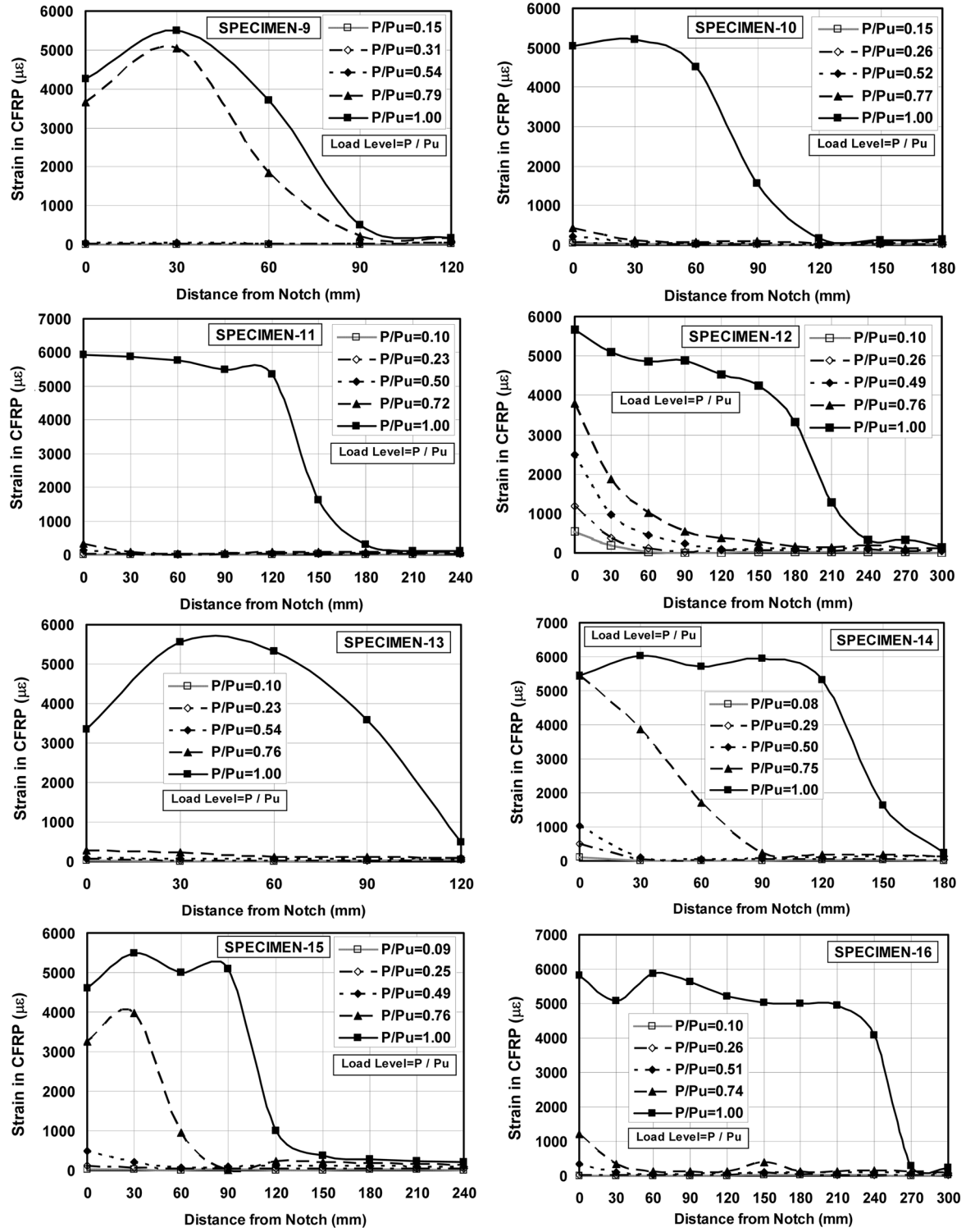
Fig. 8 Strain distribution along the CFRP sheet
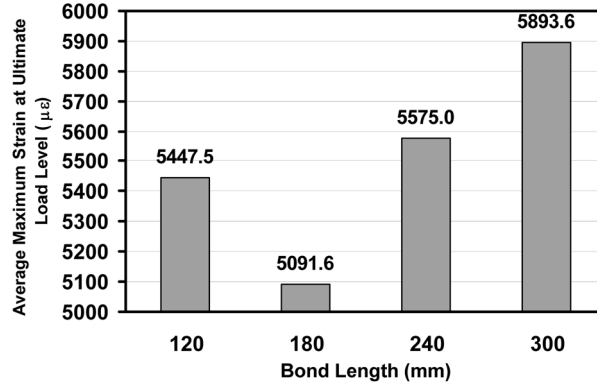
Fig. 8 Continued

Fig. 9 Effect of bond length

mean strain values of the specimens with a concrete compressive strength of 25 MPa measured at ultimate load level was 6% higher than the specimens with a concrete compressive strength of 15 MPa. Again the mean strain values of the specimens with CFRP sheet width 100 mm are 5% higher than the specimens with CFRP sheet width 50 mm. With the increase of the CFRP sheet bonding length the maximum mean strain values increased. But the strain values in the Specimens 2 and 6 with a bond length of 180 mm are smaller than the specimens with a bond length of 120 mm, due to the fact that the specimens failed when the adhesive concrete interface reached its shear capacity. The variation of the strain values with bond length are given in Fig. 9.

Eq. (1) is a proposed formula to calculate the effective bonding length of CFRP sheet with the known parameters of concrete compressive strength and the CFRP sheet thickness and modulus of elasticity (Chen and Teng 2001).

$$L_e = \sqrt{\frac{E_{CFRP} \times t_{CFRP}}{\sqrt{f_C}}} \tag{1}$$

The effective bond length of CFRP is calculated as 84.6 mm for the concrete with compressive strength of 15 MPa and 74.5 mm for the concrete with compressive strength of 25 MPa. The study of the strain distributions obtained from the experiments of CFRP reinforced concrete specimens showed that the effective CFRP sheet length that transfers the strain to the concrete is 131.3 mm in average for the concrete with compressive strength of 15 MPa and 161.3 mm in average for the concrete with compressive strength of 25 MPa, which is 23% longer than the 15 MPa cases. These values are calculated by taking average for the two experimental series. Effective CFRP strip length of Specimens 1 to 8 with 15 MPa concrete compression strength are changed between 60 to 210 mm and the same parameter are changed between 90 to 270 mm for the Specimens 9-16 with 25 MPa concrete compression strength. This variation also stems from the experimental parameters such as the total CFRP bond length and the width of strip. These are much higher than the predicted results from Eq. (1). The width of the sheet was also influencing the effective bonding length. The specimens with 100 mm sheet width have 17% higher bond length than the ones with 50 mm sheet width.

3.3 Comparison of experimental and analytical results

In this section a widely used analytical approach (Chen and Teng 2001) is compared with the experimental ultimate loads. Experimental and analytical ultimate loads and their ratios are given in Table 5. Empirical Eqs. (2), (3) and (4) which had been developed from a near-end supported (NES) single shear pull tests was used for comparison.

$$\beta_w = \sqrt{\frac{2 - b_{CFRP}/b_C}{1 + b_{CFRP}/b_C}} \tag{2}$$

$$\beta_1 = \begin{cases} 1 & \text{if } L_{CFRP} \geq L_e \\ \sin\frac{\pi}{2} \cdot \frac{L_{CFRP}}{L_e} & \text{if } L_{CFRP} < L_e \end{cases} \tag{3}$$

$$P_{cal} = \alpha \cdot \beta_w \cdot \beta_1 \cdot L_e \cdot \sqrt{f_c} \cdot b_{CFRP} \tag{4}$$

Eq. (2) is used for calculating width coefficient and Eq. (3) is used for calculating bond length coefficient. This is a half-empirical method. The coefficient α, which had been calculated by Chen and Teng (2001) from a regression analysis of some experimental findings was taken as 0.427 in this study.

In Table 5, it could be noticed that all of the experimental ultimate loads are higher than the

Table 5 Comparison of experimental and analytical results

Specimen No	Experimental ultimate load (kN)	Analytical ultimate load (kN)	*Ratio
1	9.3	7.8	1.19
2	8.8	7.8	1.12
3	8.9	7.8	1.14
4	8.7	7.8	1.11
5	14.2	12.5	1.13
6	15.0	12.5	1.20
7	14.1	12.5	1.13
8	13.5	12.5	1.08
9	9.6	8.9	1.08
10	8.9	8.9	1.00
11	9.3	8.9	1.05
12	10.1	8.9	1.14
13	14.5	14.2	1.02
14	14.4	14.2	1.01
15	16.9	14.2	1.19
16	14.6	14.2	1.03

*Ratio of experimental ultimate load capacity to analytical ultimate load capacity

analytical ultimate loads by approximately 10%. The difference is because of bond length which is important in the equation and the empirical formula was obtained from another kind of experimental setup. The experimental effective CFRP bond lengths which were calculated from the strain distributions of the specimens are higher than the analytical results. This is considered to be the main reason for higher ultimate loads in experimental values.

4. Conclusions

In this study the strain distributions between CFRP sheets bonded on to notched concrete beams are studied. Main variables of this study are concrete compressive strength, bond length and CFRP width. The results that are obtained from 16 specimens are summarized below.

1. The specimens are casted with notches for modeling a crack in concrete beams. Strain distribution on CFRP sheets is considerably affected by the notch. The strain distribution increases and reaches its maximum value near the notch mouth tip like the strain values.

2. CFRP sheet width is the most influential variable on ultimate load values compared to bond length and concrete compressive strength.

3. All specimens except 1, 2 and 6 failed from debonding of CFRP with concrete. It is observed that this case occurred more than the case in which specimens failed with failure of epoxy resin. Also strain values are higher in debonding of CFRP with concrete than epoxy resin failure cases.

4. In the debonding of CFRP with concrete cases, the thickness of debonded concrete increases near the notch mouth tip, and in the other end of CFRP. Debonding thickness depended on the strain values at those points of CFRP.

5. The variables studied in this paper had almost the same effect on the strain distributions. Increasing the concrete strength and CFRP sheet width increased the strain values by 6% at maximum ultimate load.

6. Measured maximum strains from the CFRP strips are significantly affected by the failure modes of the specimens. Measured maximum strains from the specimens that are failed due to exceeding shear strength of epoxy itself are lower than that of specimens failed due to exceeding shear strength of concrete.

7. As the bond length of CFRP strips are increased measured maximum strains are also increased. This result is changed due to failure mode only. For this reason average maximum strain value from the CFRP strips with 180 mm bond length is found to be less than that of CFRP strips with 120 mm bond length.

8. The strain values increased gradually up to 50% of the ultimate load and after this point the strain values increased rapidly.

9. In the specimens with concrete compressive strength of 25 MPa, the effective bond lengths are 23% longer than the specimens with concrete compressive strength of 15 MPa.

10. CFRP sheet width has an increasing effect on the effective strain distribution. The specimens with 100 mm sheet width have 17% longer effective bond length than the ones with 50 mm wide sheet.

11. Experimental ultimate loads are higher than the analytical ultimate loads by approximately 10%. The difference is created because of the bond length which is important in the equation. The experimental effective bond lengths which were calculated from the strain distributions of the specimens are longer than the analytical results. This is considered to be the main reason for higher ultimate loads observed in experiments.

12. The equations suggested by Chen and Teng (2001) can be used for the preliminary design phase

for calculating bond strength under induced axial loads due to applied bending loads. But for final design phase, a new equation should be extracted from experimental data for simulating the behavior more correctly under this type of loading.

References

Bizindavyi, L. and Neale, K.W. (1997), "Experimental and theoretical investigation of transfer lengths for composite laminates bonded to concrete", *Proceedings of the Annual Conference of Canadian Society for Civil Engineering*, Vol. 6: Structures-Composites Materials, Structural Systems, Telecommunications Towers, Sherbrooke, Québec.

Bizindavyi, L. and Neale, K.W. (1999), "Transfer lengths and bond strengths for composites bonded to concrete", *J. Compos. Constr.*, **3**(4), 153-160.

Brosens, K. and van Gemert, D. (1997), "Anchoring stresses between concrete and carbon fiber reinforced laminates, Non-metallic (FRP) reinforcement for concrete structures", *Proceedings of the Third International Symposium*, vol. 1, Japan Concrete Institute, Sapporo.

Chajes, M.J., Finch, Jr. W.W., Januszka, T.F. and Thomson, Jr. T.A. (1996), "Bond and force transfer of composites material plates bonded to concrete", *ACI Struct. J.*, **93**(2), 209-217.

Chajes, M.J., Januszka, T.F., Mertz, D.R., Thomson, Jr. T.A. and Finch, Jr. W.W. (1995), "Shear strengthening of reinforced concrete beams using externally applied composite fabrics", *ACI Struct. J.*, **92**(3), 295-303.

Chen, J.F. and Teng, J.G. (2001), "Anchorage strength models for FRP and steel plates bonded to concrete", *J. Struct. Eng-ASCE*, **127**(7), 784-791.

Chen, J.F. and Teng, J.G. (2003), "Shear capacity of FRP strengthened RC beams: FRP debonding", *Constr. Build Mater.*, **17**(1), 27-41.

De Lorenzis, L., Miller, B. and Nanni, A. (2001), "Bond of fiber-reinforced polymer laminates to concrete", *ACI Mater. J.*, **98**(3), 256-264.

Fukuzawa, K., Numao, T., Wu, Z., Yoshizawa, H. and Mitsui, M. (1997), "Critical strain energy release rate of interface debonding between carbon fibre sheet and mortar, Non-metallic (FRP) reinforcement for concrete structures", *Proceedings of the Third International Symposium*, Vol. 1, Japan Concrete Institute, Sapporo.

Hiroyuki, Y. and Wu, Z. (1997), "Analysis of debonding fracture properties of CFS strengthened member subject to tension, Non-metallic (FRP) reinforcement for concrete structures", *Proceedings of the Third International Symposium*, Vol. 1, Japan Concrete Institute, Sapporo.

Jayaprakash, J., Abdul Samad, A.A., Abbasovich, A.A. and Abang Ali, A.A. (2007), "Repair of precracked RC rectangular shear beams using CFRP strip technique", *Struct. Eng. Mech.*, **26**(4), 427-439.

Kobatake, Y., Kimura, K. and Ktsumata, H. (1993), "A retrofitting method for reinforced concrete structures using carbon fibre", *Fiber-reinforced-plastic (FRP) Reinforcement for Concrete Structures: Properties and Applications* (Ed. Nanni, A.), Elsevier Science, The Netherlands.

Maeda, T., Asano, Y., Ueda, T. and Kakuta, Y. (1997), "A study on bond mechanism of carbon fiber sheet, Non-metallic (FRP) reinforcement for concrete structures", *Proceedings of Third International Symposium*, Japan Concrete Institute, Sapporo.

Mohamed Ali, M.S., Oehlers, D.J. and Bradford, M.A. (2002), "Interaction between flexure and shear on the debonding of RC beams retrofitted with compression face plates", *Adv. Struct. Eng.*, **5**(4), 223-230.

Mohamed Ali, M.S., Oehlers, D.J. and Bradford, M.A. (2001), "Shear peeling of steel plates bonded to the tension faces of RC beams", *J. Struct. Eng-ASCE*, **127**(12), 1453-1460.

Neubauer, U. and Rostásy, F.S. (1997), "Design aspects of concrete structures strengthened with externally bonded CFRP plates", *Proceedings of Seventh International Conference on Structural Faults and Repairs*, Vol. 2, ECS Publications, Edinburgh.

Oehlers, D.J. and Moran, J.P. (1990), "Premature failure of externally plated reinforced concrete beams", *J. Struct. Eng-ASCE*, **116**(4), 978-995.

Oehlers, D.J., Park, S.M. and Mohamed Ali, M.S. (2003), "A structural engineering approach to adhesive bonding of longitudinal plates to RC beams and slabs", *Compos. Part A*, **34**(12), 887-897.

Smith, S.T. and Teng, J.G. (2002a), "FRP-strengthened RC beams-I: review of debonding strength models", *Eng. Struct.*, **24**(4), 385-395.

Smith, S.T. and Teng, J.G. (2002b), "FRP-strengthened RC beams-II: assessment of debonding strength models", *Eng. Struct.*, **24**(4), 397-417.

Smith, S.T. and Teng, J.G. (2003), "Shear-bending interaction in debonding failures of FRP-plated RC beams", *Adv. Struct. Eng.*, **6**(3), 183-199.

Swamy, R.N., Jones, R. and Charif A. (1986), "Shear adhesion properties of epoxy resin adhesives", *Proceedings of International Symposium on Adhesion between Polymers and Concrete*, London.

Taljsten, B. (1997), "Defining anchor lengths of steel and CFRP plates bonded to concrete", *Int. J. Adhes. Adhes.*, **17**(4), 319-327.

Teng, J.G., Chen, J.F., Smith, S.T. and Lam, L. (2002), *FRP-strengthened RC Structures*, Wiley, Chichester.

Teng, J.G., Smith, S.T., Yao, J. and Chen, J.F. (2003), "Intermediate crack-induced debonding in RC beams and slabs", *Constr. Build Mater.*, **17**(6-7), 447-462.

Van Gemert, D. (1980), "Force transfer in epoxy-bonded steel-concrete joints", *Int. J. Adhes. Adhes.*, **1**(2), 67-72.

Yao, J., Teng, J.G. and Chen, J.F. (2005), "Experimental study on FRP-to-concrete bonded joints", *Compos. Part B-Eng.*, **36**(4), 99-113.

Ziraba, Y.N., Baluch, M.H., Basunbul, A.M., Azad, A.K., Al-Sulaimani, G.J. and Sharif, I.A. (1995), "Combined experimental-numerical approach to characterization of steel-glue-concrete interface", *Mater. Struct.*, **28**(9), 518-525.

Conversion factors

1 mm = 0.039 in
$1 \text{ mm}^2 = 0.00152 \text{ in}^2$
1 kN = 0.2248 kips
1 MPa = 145 psi

Notations

a : Shear span of beam (mm)
b_C : Beam web width (mm)
b_{CFRP} : CFRP sheet width (mm)
d : Effective height of cross section (mm)
E_{CFRP} : Elastic modulus of CFRP (MPa)
f_c : Compression strength of concrete (MPa)
L_{CFRP} : Bond length of CFRP sheet (mm)
L_e : Effective bond length (mm)
P : Applied load (kN)
P_{cal} : Calculated ultimate load (kN)
P_U : Experimental ultimate load (kN)
t_{CFRP} : Thickness of CFRP (mm)
α : Regression coefficient of Chen and Teng (2001) experimental values
β_w : Beam web and CFRP sheet width correction coefficient
β_l : Bond length and effective length of CFRP sheet correction coefficient